JTTEE5 16:128–139
DOI: 10.1007/s11666-006-9000-9
1059-9630/$19.00 © ASM International

Peer Reviewed

Model-Based Expert System for Design and Simulation of APS Coatings

Florin-Iuliu Trifa, Ghislain Montavon, and Christian Coddet

(Submitted December 17, 2005; in revised form July 26, 2006)

This article aims at presenting an expert system to assist the design and the simulation of 2-D shapes of alumina-titania (i.e., Al_2O_3-13 wt.% TiO_2) Atmospherically Plasma Sprayed (APS) coatings. Indeed, the expert system derives from a spray deposition mathematic model resulting from experiments. The varied processing parameters were the geometric and the kinematics parameters, mainly, such as: the relative speed gun-substrate, the spray distance, the spray angle, the relative positioning powder injector-spray gun trajectory, the number of passes and the powder feed rate. The variations of the geometry and some of the structural parameters were analyzed relatively to the aforementioned varied parameters. Thus, a large set of spray pattern parameters was designed. This set considers mostly the spray pattern geometry. All the relationships between the processing parameters and the spray pattern parameters were hence grouped in a spray deposition model. The second step of this work consisted in optimizing the robotic (i.e., spray gun) trajectory using a robotic code, which permits a realistic simulation of the spray gun speed and its inertia. Using this simulation software, a trajectory file was built. In the third step of the work, an expert system was developed by combining the spray deposition model with the trajectory. The tasks of the expert system are: (1) to assist the user in designing the coatings by selecting the processing parameters and (2) to simulate the coating shapes by integrating the gun trajectory.

Keywords alumina-titania, atmospheric plasma spraying, coating design and simulation, expert system, robotic simulation, spray pattern model

1. Introduction

Thermal spraying permits to cover parts of a large variety of morphologies and dimensions (e.g., turbine blades, medical implants, cylinders for rolling mills, etc.) to confer them specific in-service properties.

The traditional way to program the robot trajectory is on-line programing. This signifies that the robot duplicate a trajectory that was ''taught'' to it previously. For complex parts such as turbine blades for example, the programing time can become relatively long (a few days to a few weeks in certain cases) and the trajectory is not fully optimized. Moreover, the resulting spray pattern properties are not taken into account explicitly.

This work considers a different approach as it is based on the optimization of the trajectory by off-line programing using robot simulation software. Then, this trajectory is interfaced with a spray deposition model to predict the coating geometry to reach a better process optimization.

Several published works considered relatively similar subjects than the one developed in this study (Ref 1-4). The nature of these works was nevertheless limited to:

- either the determination of the spray pattern properties as a function of different processing parameters. The correlations thus found were not integrated into robot simulation to optimize the coating or spray pattern properties
- or the study of the spray pattern geometry (mostly its thickness) as a function of the kinematics parameters; these studies were interfaced with a robot simulation software but neglecting most of the time the properties of spray pattern (i.e., hardness, stiffness, etc.)

This study aims at designing an expert system integrating a spray deposition model to a robot trajectory. The studied case considered alumina-titania powder (Al_2O_3-13 wt.% TiO_2) atmospherically plasma sprayed (APS). A large number of experiments were carefully conducted to quantify the relationships between the processing parameters and some spray pattern characteristics. Unlike most of the other studies, the developed spray deposition model considers the spray pattern geometry but also some spray pattern structural properties. The studied processing parameters were:

- the number of passes
- the scanning step
- the relative speed (spray gun—substrate)
- the spray distance
- the spray angle

F.-I. Trifa, G. Montavon, and **C. Coddet,** LERMPS, Université de Technologie de Belfort-Montbéliard, Belfort Cedex, 90010, France; **F.-I. Trifa,** ALSTOM CSR, Zentralstrasse 40, Birr, 5242, Switzerland; and **G. Montavon,** SPCTS-UMR CNRS 6638, Faculté des Sciences et des Techniques, Université de Limoges, 123 avenue Albert Thomas, Limoges Cedex, 87060, France. Contact e-mail: ghislain.montavon@unilim.fr

Nomenclature	
α [deg]	spray angle
η [%]	spray deposition efficiency
σ [mm]	standard deviation of the pattern width
$A(n)$ [mm^2]	pattern area after n passes
A [mm^2]	pattern area
APS	Atmospheric Plasma Spraying
d [mm]	spray distance
E [GPa]	coating apparent Young modulus
$H(n)$ [mm]	spray pattern height after n passes
H [mm]	spray pattern height
HK [GPa]	coating Knoop hardness
K [dimensionless]	kurtosis (pointedness) of the pattern waviness profile
$L_{\frac{u}{2}}$ [mm]	pattern width at its half height
n	number of passes
Off [mm]	offset of the pattern peak relative to torch centerline axis
Off spray [mm]	lateral movement (out of the part) distance of the spray gun
PF [g/min]	powder mass flow rate
por [%]	pattern porosity level
Ra [μm]	pattern average roughness
Re [dimensionless]	particle Reynolds number upon impact
Ry max [μm]	pattern maximum peak-to-valley roughness
Sk [dimensionless]	skewness (asymmetry) of the pattern waviness profile
SS [mm]	scanning step
T [°C]	substrate temperature
v [mm/s]	spray gun speed relative to substrate
We [dimensionless]	particle Weber number upon impact

Table 1 Processing parameters

Constant parameters		Variable parameters	
Arc current intensity	530 A	Spray angle	30-90 °C
Argon flow rate	40 SLPM	Spray distance	115-135 mm
Hydrogen flow rate	10 SLPM	Spray velocity	100-400 mm/s
Feedstock rate	18 g/min	Scanning step	0-10 mm
Carrier gas flow rate	3.2 SLPM	Number of passes	2-12 passes
Injector diameter	1.5 mm	Injection position	parallel, perpendicular

For a F4 type spray gun equipped with a 6 mm diameter nozzle.

- the powder flow rate
- the direction of the powder injection relative to the gun trajectory

The plasma gun power parameters (i.e., plasma arc current intensity, composition and flow rate of the plasma gases) were kept constant to reference values (Table 1). So, it was assumed in a first analysis that the treatment of the feedstock by the plasma jet was almost constant and the noticed effects were exclusively related to the varied parameters.

2. Experimental Procedure

A commercial Al_2O_3-13 wt.% TiO_2 (Metco 130*) powder of +15 to −53 μm particle size distribution was processed by APS and spray patterned on stationary S 235 steel plate substrates ($120 \times 60 \times 5$ mm^3). Prior to spraying, the feedstock powder was dried at about 80 °C for at least 72 h and then homogenized. The substrates were cleaned by immersion in alcohol vapors and manually grit blasted with white corundum (i.e., α-Al_2O_3 of 500 μm, average diameter) to generate an average roughness of 4 μm, average value.

An atmospheric plasma gun (Sulzer-Metco F4**) was fixed on an ABB*** IRB 2400 robot. Most of the time, coatings were consisting in one spray pattern resulting from several gun passes in front of the same location of the substrate. This approach permits to estimate the influence of the processing parameters and to measure the spray pattern characteristics with a fairly high accuracy. The experimental set-up is illustrated in Fig. 1 and the processing parameters are listed in Table 1.

The experimental protocols used to quantify the results included (Ref 5-7):

- Laser profilometry and contact profilometry to quantify the bead geometry
- Roughness measurements to quantify the bead surface characteristics
- Image analysis to study the bead microstructure
- Microhardness measurements to quantify their mechanical response

Precise devices and reliable experimental protocols were implemented to insure the reproducibility of the results analyzed mostly from a statistical point of view. For bead geometry, 20 profiles measured by laser profilometry with a scanning step of 0.2 mm were averaged to calculate the mean profile. The roughness characteristics (i.e., Ra and Ry max) resulted from 20 adjusted measurements with a 0.8 mm cut-off along the bead profile. Concerning the Knoop microhardness, 8 random spaced indentations were considered for each bead section. The spray pattern porosity levels were assessed from three randomly located images for each section using the Scion Image (http://www.scioncorp com) software and the Delesse stereological protocol.

Figure 2 displays a typical bead fitted geometry (by a Gaussian approximation) and its microstructure (in cross-section). The porosity of typical 10-pass bead

*Sulzer Metco Holding AG, Zürcherstrasse 12, CH-8401 Winthertur, Switzerland.
**F4 is a series of plasma guns for air/vacuum spraying. F4 is marketed by Sulzer Metco Holding AG.
***ABB Automation Technology Products AB, Drakegatan 6, 41250 Gothenburg, Sweden.

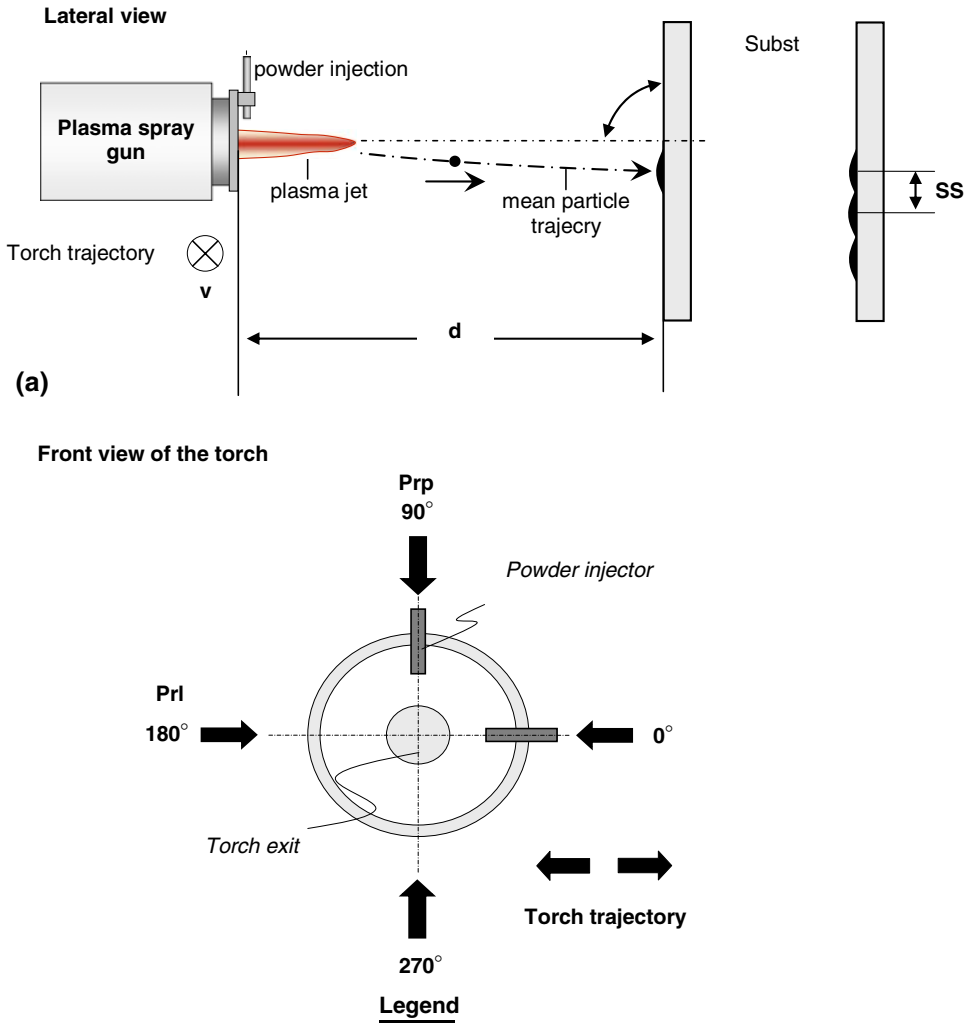

Fig. 1 Schematic view of experimental parameters

microstructure sprayed with standard parameters is approximately 0.08% with a standard deviation of 0.03%.

3. Spray Deposition Model and Database

The spray deposition model is a set of mathematical functions based on experiments. The spray deposition model considers on the one hand the spray pattern geometry and on the other hand the spray pattern microstructural properties.

3.1 Spray Pattern Geometry

Hereafter are synthesized the major results concerning the spray pattern geometry (Ref 5-9):

- In a transversal section, the beads present, whatever the operating parameters, a Gaussian shape (R^2 = 0.95-0.99). Size and shape indicators were defined to quantify these geometries.
- to obtain a significant spray pattern thickness to be measured, several passes were superimposed on top of each other. Then, thickness and area/pass were calculated *a posteriori* from the spray pattern final thickness and the number of passes. A homothetic growth of the spray pattern was hence observed (i.e., a linear increase of spray pattern area and height with the number of passes). For example, the spray pattern height, $H(n)$, and area, $A(n)$, after n passes in the case of a powder injection parallel to the torch trajectory are quantified as follows:

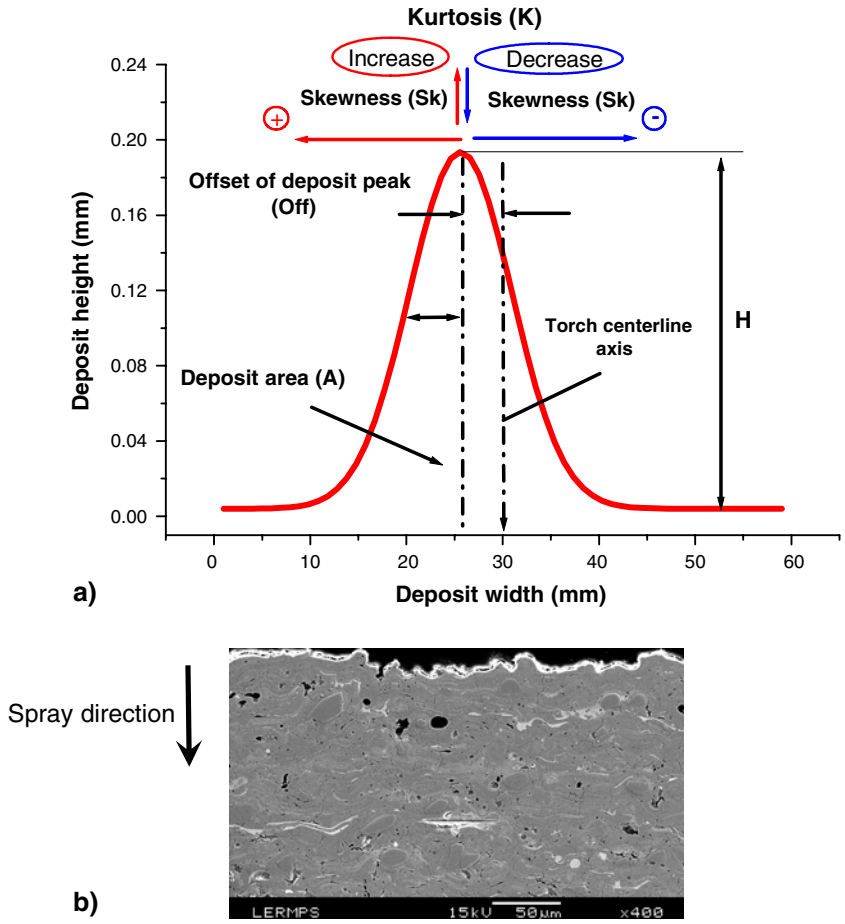

Fig. 2 Typical spray pattern: (a) fitted profile (one bead, 10 passes); (b) typical microstructure

$$H(n)\,[\text{mm}] = n \times 0.019; \quad R^2 = 0.870 \qquad \text{(Eq 1)}$$

$$A(n)\,[\text{mm}^2] = n \times 0.245; \quad R^2 = 0.828 \qquad \text{(Eq 2)}$$

The spray pattern roughness, the spray pattern width and its position do not change significantly with the number of passes when spray pattern is continuous.

- The spray pattern width at its half height ($L_{\frac{H}{2}}$) as a function of spray angle (α) in the case of a powder injection parallel to the torch trajectory can be computed as follows:

$$L_{\frac{H}{2}}\,[\text{mm}] = 19.143 - 0.089 \times \alpha; \quad \alpha\,[\text{deg}]; \quad R^2 = 0.772 \qquad \text{(Eq 3)}$$

When the spray angle decreases from 90° to 45°, the spray pattern center of mass position translates by 2.5 mm and the spray pattern height roughly halves. The spray pattern roughness increases also when the spray angle decreases.

- Figure 3 displays the spray pattern height evolution vs. the spray gun speed relative to the substrate. Even if a linear relationship can be observed for speed values superior to 200 mm/s, an exponential relationship is more appropriate to fit the overall range of values. Such a non linear behavior is not a violation of the mass conservation principle, since there is of course no more mass in the final spray pattern than the feedstock mass than it was injected in the plasma plume. The

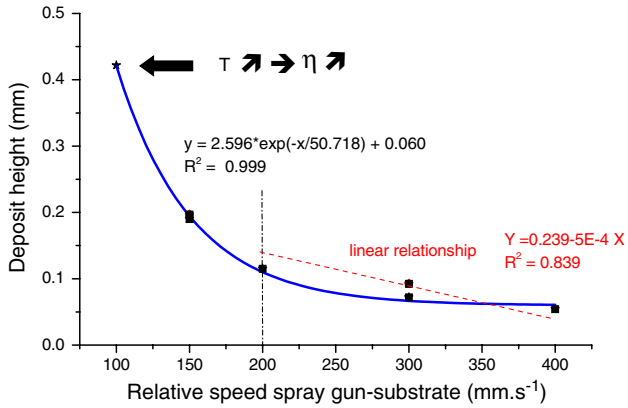

Fig. 3 Spray pattern height vs. spray gun-substrate relative speed

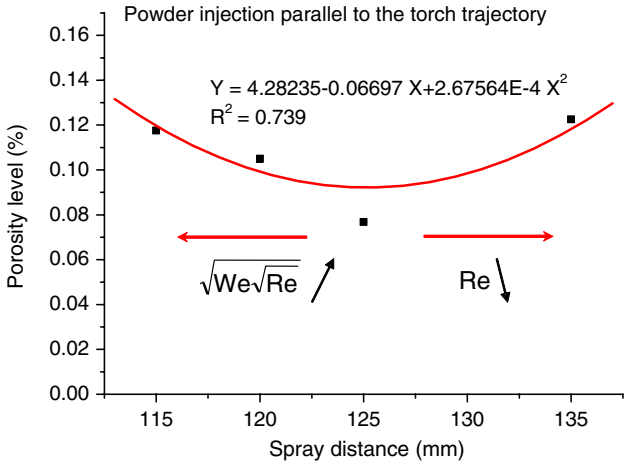

Fig. 4 Spray pattern porosity level vs. spray distance

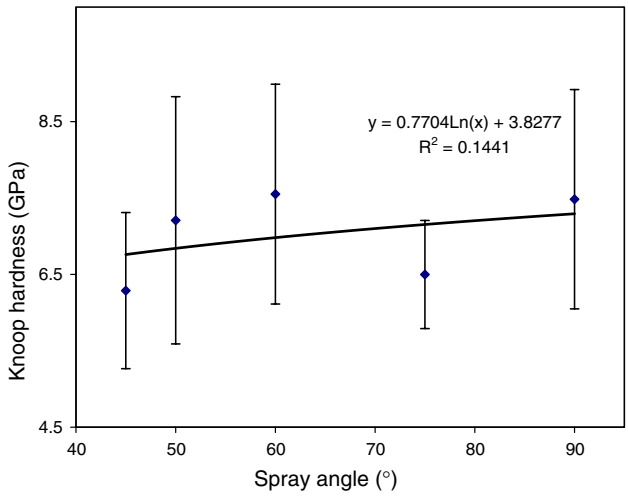

Fig. 5 Knoop hardness vs. spray angle

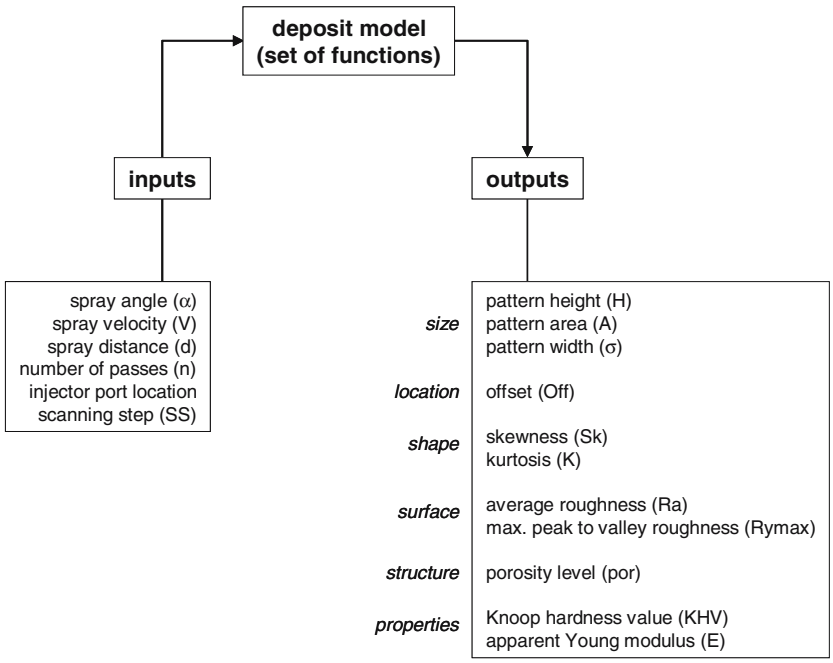

Fig. 6 Deposition model concept

explanation consists very likely in higher feedstock spray deposition efficiency at low spray gun speeds due to an increase in the substrate temperature. Exponential relationships between the spray gun speed and the spray pattern area were also observed.

- The spray distance modifies the spray pattern width (i.e., it increases when the spray distance increases since the spray pattern widens), its height, its area and the position of the spray pattern mass center.
- The scanning step controls the overlapping degree of the successive beads; a linear increase in the spray pattern height when the scanning step decreases was quantified. The waviness of the spray pattern decreases when the scanning step decreases.
- Two positions between the powder injection and the spray gun trajectory were systematically studied: parallel and perpendicular. It was found that the spray patterns sprayed with a parallel injection port are larger (by 15-20%) than those produced with a perpendicular injection port, the other parameters remaining similar. The tolerance of the angular positioning of the powder injector should be precise (1°-2° maximum) as a 5° tolerance can translate by about 2 mm the spray pattern center of mass. So, the precision of the powder

injector location is of prime importance for a proper calibration of spray patterns on the part.

3.2 Spray Pattern Structural Properties

The second part of the spray deposition model concerns the spray pattern structural properties. Hereafter are presented the major results:

- A limited increase of the spray pattern porosity with the number of passes was observed, considering that the deposit is continuous (i.e., deposit thicker as 40-50 μm), as displayed in Ref 5. When the number of passes increases from 8 to 12 passes, the porosity increases from about 0.06% to about 0.08% (Ref 5).
- Although the spray pattern porosity level is rather low in all cases (less than 1%), a variation is however detectable. For a 10-pass deposit sprayed with standard parameters, the typical porosity is about 0.08%. Even if such a porosity value may seem low, all samples were optimally prepared by automatic polishing with similar parameters, analyzed identically and the values were carefully measured and verified several times. Figure 4 illustrates the relationship between the spray distance and the pattern porosity level. A minimal porosity value is reached at the spray distance of about 125 mm (i.e., the ''nominal'' spray distance in the present study). The extra porosity for distances lower than 125 mm is likely induced by a higher value of the impinging particle Sommerfeld criteria that induces more particle splashing at impact and so extra porosity. *A contrario*, at spray distances higher than 125 mm, the particle average velocity lowers (so lowers the *Re*) and more porosity develops due to lower flattening degrees. The existence of a similar evolution of the porosity level with the spray distance was highlighted also by Gowri et al., in the case of alumina deposited by APS (Ref 10). They reported also a minimum porosity level for a spray distance of about 120-125 mm. The following relationship quantifies the Knoop hardness value as a function of the spray distance (d):

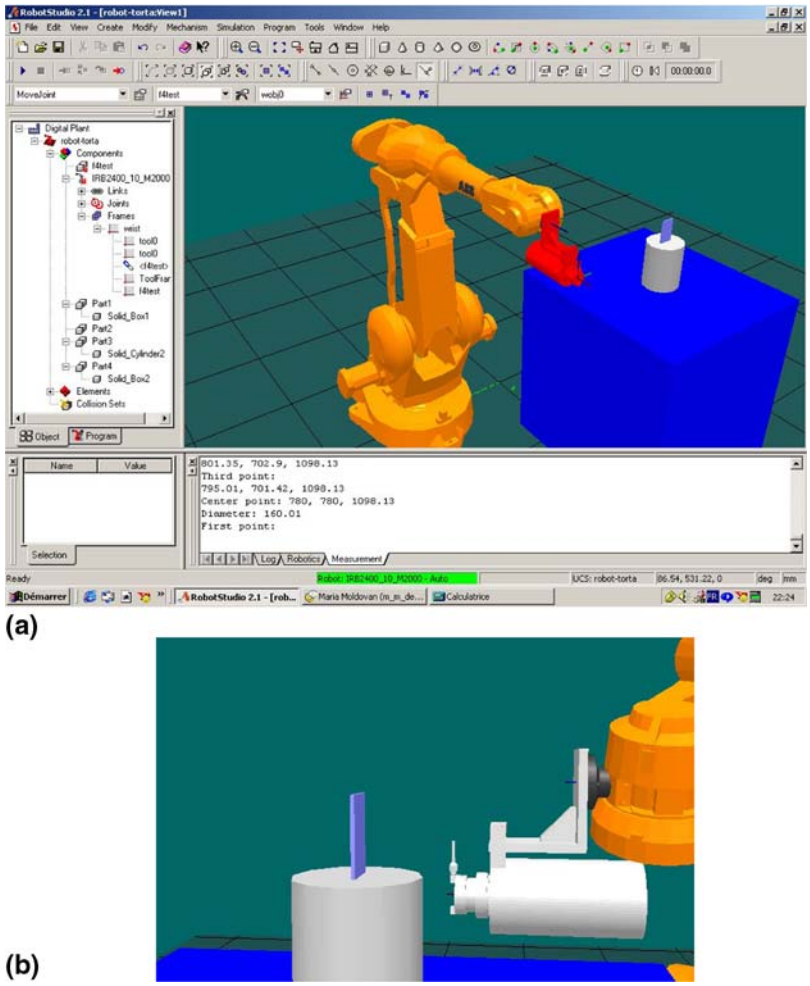

Fig. 7 Robotic simulation: (a) general view; (b) lateral view of torch

$$HK[GPa] = -457.44405 + 7.31168 \times d - 0.02868 \times d^2; \quad d\,[\text{mm}]; \quad R^2 = 0.407 \qquad \text{(Eq 4)}$$

- Figure 5 displays the relationship of the Knoop hardness values vs. the spray angle: a decrease of 19% in the spray pattern hardness is noticed when the spray angle decreases from 90° to 45°. This decrease in the deposit hardness is very likely caused by an increase in the porosity level (84%). In that case, the bead roughness increases also by 16% for *Ra* and 12% for *Ry* max. This extra roughness participates also to the development of more pores in the deposits because of the shadow effect on the incoming particles (Ref 6)

All the aforementioned results were synthesized within a data base to architecture the spray deposition model which describes the characteristics of the spray patterns as a function of the studied operating parameters. This model is composed of a set of mathematical functions and its concept is illustrated in Fig. 6.

4. Robotic Trajectory Simulation

The working environment (i.e., spray booth) hazards and the need to cover complex parts require the use of robots (Ref 11). The robot trajectory and therefore the one of the torch should be programed before execution. Two ways of programing robot trajectory are currently encountered (Ref 12-14):

- On-line programing which is carried out on the production site by leading the tool on target points in order to save in the robot memory the data consisting in the axis actuator positions and orientations. On-line programing is simple, does not require a special training of the operator but tends to be long for complex parts, imprecise and involves a robot shut down during programing task.
- Off-line programing is performed outside the production cell, on a computer using a simulation software. It permits to define an optimum trajectory based on CAD model of the parts and real robot performances. Off-line programing minimizes hence the robot shutdown

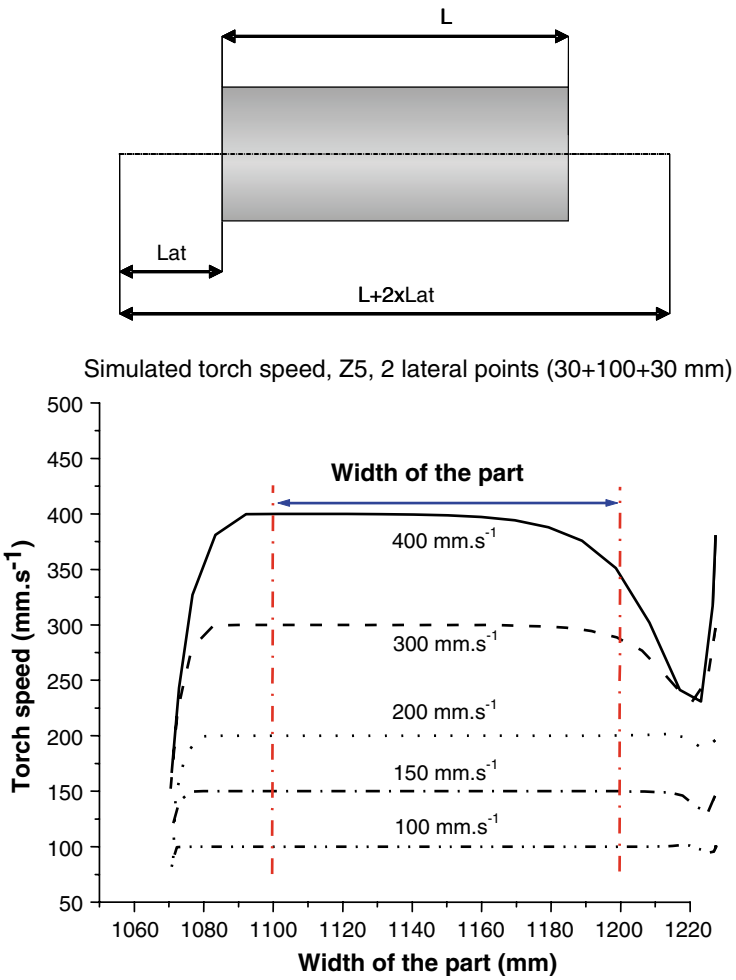

Fig. 8 Torch trajectory: (a) target points; (b) real speed vs. programed speed for one pass

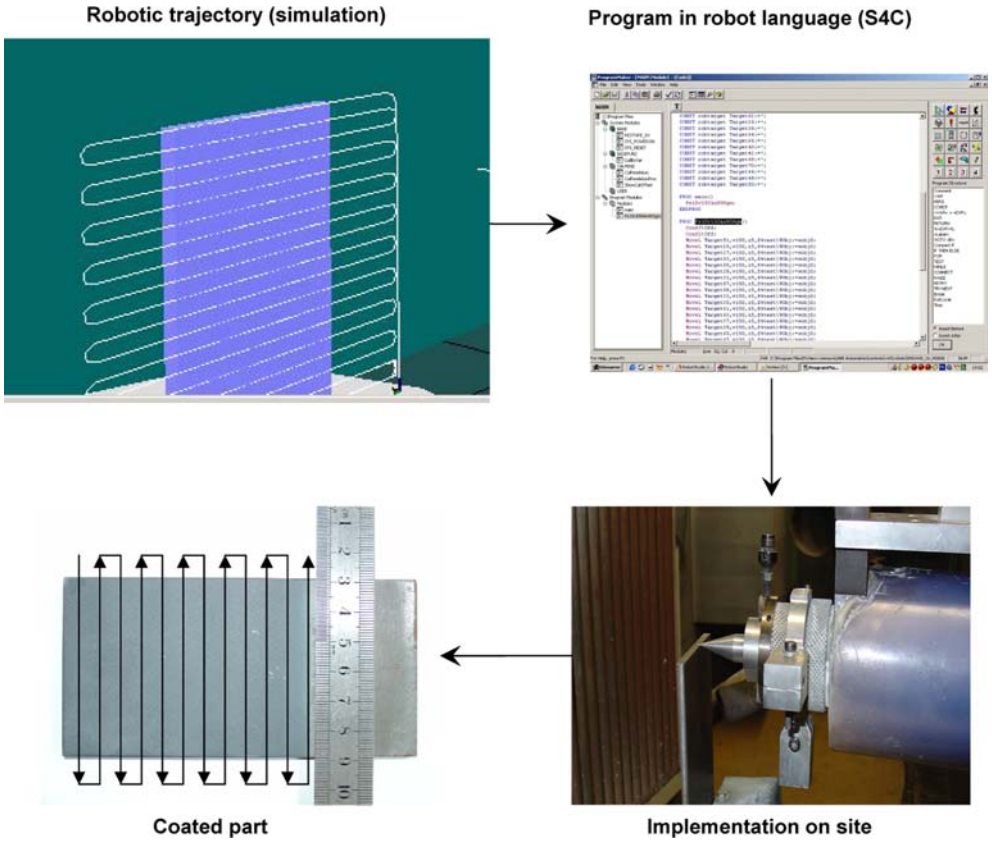

Fig. 9 Implementation of spray gun trajectory to coat the part

Off-line programing was considered in this study. The software implemented was the commercially available Robot Studio package from ABB (also the producer of the robot considered in this study). It integrates the dynamic models of real robots, including their inertia. The simulated trajectory can be used in two ways: as an executive program generated during simulation in robot language or as a trajectory file mentioning all the tool positions vs. time.

Figure 7 shows a typical virtual robotic cell from Robot Studio. The target points have to be defined as well as the lateral movement distance. It is necessary to guarantee a uniform speed of the spray gun over the part since stopping the spray gun over the part cannot be acceptable. Based on the simulated trajectory, the ''real'' speed of the spray gun taking into account the gun inertia can be simulated as displayed in Fig. 8. It can be noticed in this figure the comparison between the programed speed and ''real'' speed for a common value of lateral movement distance (i.e., 30 mm). For this robot type (ABB 2400), this spray gun (F4) and this lateral movement distance (30 mm), it can be noticed that a uniform speed over the substrate results from programed speed values lower than 300 mm/s. However, if the speed is higher than 300 mm/s, an area of the substrate is swept with a lower speed. More matter is deposited in such a way there and more heat input is transmitted to substrate. Thus, a higher level of residual stress will likely develop in the spray pattern at this location. Therefore, the value of the lateral movement distance needs to be adjusted as a function of the gun speed and the robot characteristics in order to generate uniform coatings. The value of lateral movement distance was optimized in this study to generate uniform coatings as follows:

- for $v < 300$ mm/s, Lat = 30 mm
- for $v = 300$ mm/s, Lat = 40 mm
- for $v > 300$ mm/s, Lat = 60 mm

Figure 9 displays the implementation of an optimized multi-pass trajectory for the real robot to cover a real part. Based on the simulated trajectory, a robot program is generated and the trajectory is validated before the part is covered. So the position of the part and the trajectory of the spray gun centerline axis are precisely settled when conducting experiments.

5. Expert System

Another functionality of the Robot Studio package is to generate trajectory files where the positions and

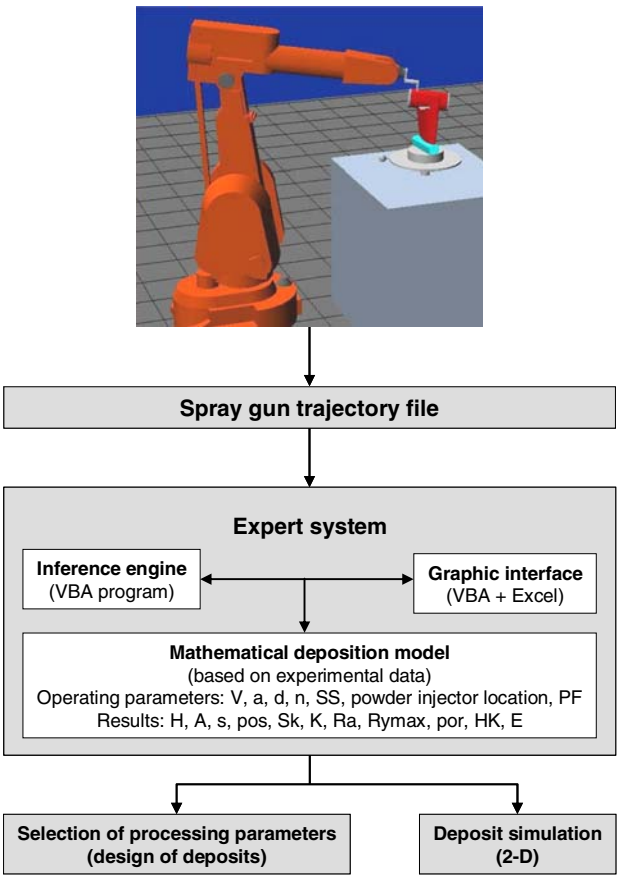

Fig. 10 Expert system concept

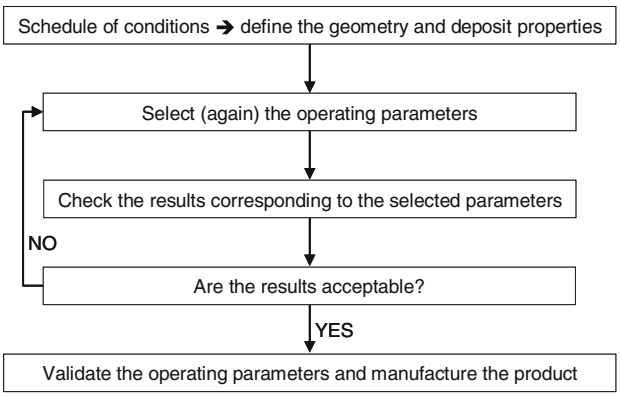

Fig. 11 Design of coatings by selecting the processing parameters

orientations of the robot axes are recorded as a function of time. Such trajectory files were defined and interfaced with the spray deposition model in an expert system written in Visual Basic for Applications (VBA). It permits the selection of the processing parameters and the simulation of the 2-D spray pattern along the robot trajectory. An expert system is a part of the artificial intelligence field. It is the product of a know-how in a particular field

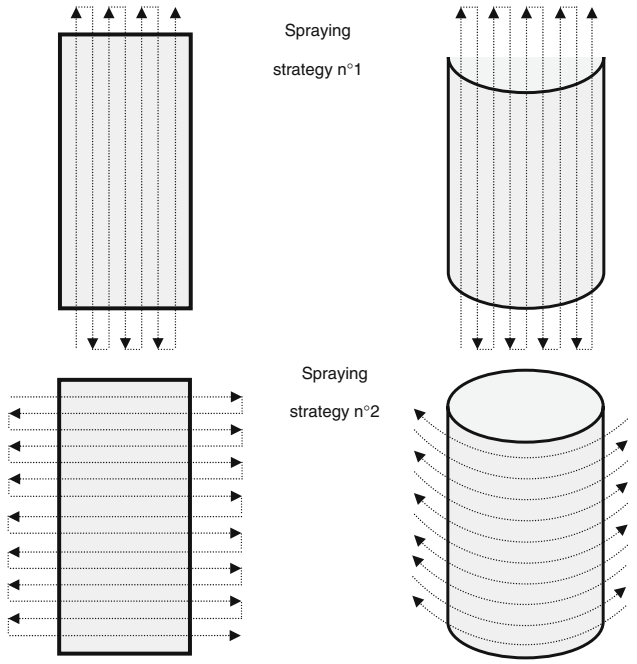

Fig. 12 Two spray strategies

and it tries to bring "know-how" where the need for an expertise is necessary. An expert system is constituted usually by three components: an inference engine (computer application), a database, and a user interface allowing the user to communicate with the system (Ref 10, 15, 16).

All the equations resulting from the mathematical spray deposition model were programed in the VBA software (Fig. 10). Figure 11 presents the concept of design of coatings by selection of processing parameters.

Figure 12 presents an example of two spray strategies implemented to generate uniform coatings by spray deposition of parallel adjacent beads spaced by a constant scanning step value (typically equal to the standard deviation σ of the bead width). The expert system permits also to draw the attention of the designer if a threshold value of the spray pattern height (i.e., corresponding indeed locally to a high level of residual stress) is trespassed by the choice of the processing parameters.

6. Comparative Results Simulation Versus Experimental

A comparison between simulated and experimental results is presented in Figure 13 which displays the spray pattern profiles in three cases: (1) one bead produced with two spray distances; (2) two adjacent beads; and (3) multibead spray pattern. It can be noticed here that the simulation offers values close to the experiments.

Three cases were especially investigated to validate the results (Table 2): (1) one bead with different processing parameters; (2) two adjacent beads; and (3) coatings

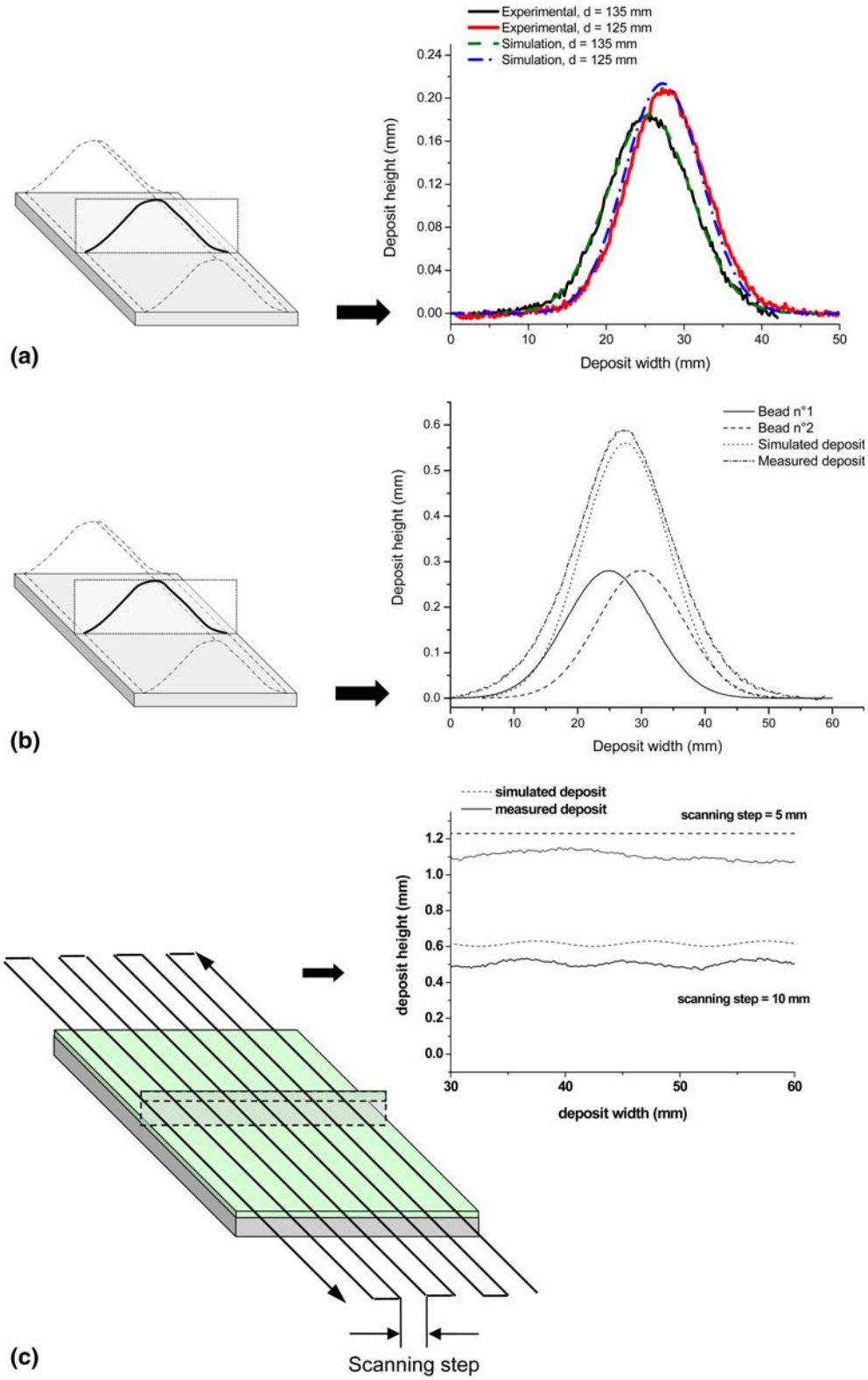

Fig. 13 Comparative examples simulation-experimental: (a) one bead; (b) two next beads; (c) multibead spray pattern

resulting from several beads. The overall average of differences between simulation and experiments is 6.5% for spray pattern height and 10.3% for spray pattern area. A fairly good agreement between simulation and experiments is hence reached and the validation can be considered as validated. Nevertheless, these misfits can result

Table 2 Synthesis of the validations: simulation vs. experimental

	Experimental		Simulation		Difference			
	H, μm	A, mm²	H, μm	A, mmP²	H, μm	H, %	A, mm²	A, %
1 Bead								
10 passes: α = 90°; *v* = 150 mm/s; *d* = 125 mm; *PF* = 18 g/min	205	2.616	213	2.647	8	3	0.031	1
10 passes: α = 45°: *v* = 150 mm/s; *d* = 125 mm; *PF* = 18 g/min	90	1.508	103	1.759	13	14	0.251	16
10 passes: α = 90°; *v* = 150 mm/s; *d* = 135 mm; *PF* = 18 g/min	184	2.484	185	2.495	1	0.5	0.011	0.4
2 Beads								
SS: 10 mm 10 passes; *v* = 150 mm/s; α = 90°; *PF* = 25 g/min	616	12.025	675	13.430	59	10	1.405	12
SS: 10 mm 10 passes; *v* = 150 mm/s; α = + 45° & −45°; *PF* = 25 g/min	567	10.869	560	9.565	7	1	1.304	12
Multibead deposits								
8 beads *SS*: 10 mm 10 passes; *v* = 150 mm/s; α = 90°; *PF* = 25 g/min	575	31.030	630	36.934	55	10	5.904	19
15 beads *SS*: 5 mm 10 passes; *v* = 150 mm/s; α = 90°; *PF* = 25 g/min	1152	56.753	1230	63.343	78	7	6.590	12
Overall mean differences	...	...	...	...	...	6.5	...	10.3

from specificities that are not yet taken into account in the expert system such as the surface roughness or the variation of the spray deposition efficiency due to local variation of the spray angle.

7. Concluding Remarks

An expert system was build based on a mathematic spray deposition model for APS sprayed Al_2O_3-TiO_2 (13 wt.%). The system takes into consideration the robot trajectory issued from a robotic simulation to simulate the spray deposition by describing the resulting 2-D shapes. The system brings also help to the user in choosing the processing parameters by presenting the results on the graphic interface and on Microsoft Excel type spreadsheet.

A fairly good agreement was obtained between the simulation and experiments. The system is at this moment dedicated to alumina-titania coatings produced by APS on plane and cylinder substrates but can be extended to other materials, processes and substrate geometries following the same developed protocol.

Acknowledgments

LERMPS-UTBM is a member of the *Institut des Traitements de Surface de Franche-Comté* (ITSFC, Surface Treatments Institute of Franche-Comté), France.

References

1. M. Friis, C. Persson, Process window for plasma spray processes, pp. 1313-1319 of *Thermal Spray 2001: New Surfaces for a New Millennium*, C.C. Berndt, K.A. Khor, and E.F. Lugscheider, Ed., May 28-30, 2001 (Singapore), ASM International p 1381
2. A. Ilyuchenko, P. Vityaz, V. Okovity, V. Abrashin, G. Gromyko, T. Veremeinko, and G. Zajac, Mathematical Model for Process Thermal Spraying Coating Formation. p 569-576 of *Thermal Spray: Practical Solutions for Engineering Problems*, C.C. Berndt, Ed., Oct 7-11 (Cincinnati, OH), ASM International, 1996, p 992
3. S. Gowri, G. Uma Shankar, K. Narayanasamy, and R. Krishnamurthy, Expert System for Process Optimization of Atmospheric Plasma Spraying of High Performance Ceramics, *J. Mat. Process. Technol.*, 1997, **63**, p 724-732
4. D. Montillet, PhD thesis (in French). Simulation et Optimisation de la Projection Plasma Robotisée (Simulation and Optimization of the Robotic Plasma Spraying). Université de Montpellier II, France, 1999
5. F.-I. Trifa, PhD thesis (in French). Modèle de Dépôt Pour la Simulation, la Conception et la Réalisation de Revêtements Elaborés par Projection Thermique: Application au cas de L'alumine—Rutile (Al_2O_3-13% TiO_2) Projetée à la Torche Atmosphérique à Plasma D'arc (Spray Pattern Model for the Simulation, Design and Manufacturing of the Thermal Spraying Coatings: Application for the Case of Alumina-Titania (Al_2O_3-13% TiO_2) Sprayed by APS). Université de Technologie de Belfort-Montbéliard, France, 2004
6. F.-I. Trifa, G. Montavon, C. Coddet, P. Nardin, and M. Abrudeanu, Geometrical Features of Plasma-Sprayed Spray Patterns and Their Characterization Methods, *Mat. Charact.*, 2005, **54**, p 157-175
7. F.-I. Trifa, G. Montavon, and C. Coddet, On the Relationships Between the Geometric Processing Parameters of APS and the Al_2O_3-TiO_2 Spray Pattern Shapes, *Surf. Coat. Technol.*, 2005, **195**, p 54-69
8. F.-I. Trifa, G. Montavon, and C. Coddet, On the Effects of the Spray Kinematics on the Spray Patterned Bead Shape and Structure of Thermal Spray Al_2O_3-TiO_2 (13 wt.%). *Thermal Spray 2004: Advances in Technology and Application*, ASM International, May 10-12, 2004 (Osaka, Japan), ASM International, 2004, p 1129
9. F.-I. Trifa, G. Montavon, and C. Coddet, Integrating a Spray Deposition Model for Off-Line Spray Tools Programing. Oral Presentation in the ITSC 2-5 May 2005, Basel, Switzerland. Thermal Spray 2005: (e-proceedings), (Pub.) DVS-Verlag GmbH, Düsseldorf, Germany, 2005
10. S. Gowri, G. Uma Shankar, K. Narayanasamy, and R. Krishnamurthy, Expert System for Process Optimization of Atmospheric Plasma Spraying of High Performance Ceramics, *J. Mat. Process. Technol.*, 1997, **63**, p 724-732
11. K.R. Abram, J. Bustamante, and R.D. Etzenhouser, Automated Metal Spray Applications. p 655-660 of *Thermal Spray Research and Applications*, T.F. Bernecki, Ed., May 20-25, 1990 (Long Beach, CA), ASM International, 1991, p 792
12. J.J. Craig, Introduction to Robotics: Mechanics and Control, 2nd ed., Addison Wesley, MA, 1989, p 464
13. R. Bonnet, PhD thesis (in French). La Projection Thermique sur des Formes Complexes: Simulation et Etalonnage du Procédé Robotisé (Thermal Spraying on Complex Shapes: Simulation and Calibration of Robotic Technique). Université de Franche-Comté, France, 2000
14. O. Legoff, PhD thesis (in French). Extraction D'attributs et Réseaux Neuronaux en Programation Hors-Ligne de Robots de Soudage (Extraction of Attributes and Neural Networks in

Off-Line Programing of Welding Robots). Ecole Centrale de Nantes, France, 1995.
15. T. Katayama, M. Akamatsu, and Y. Tanaka, Construction of PC-Based Expert System for Cold Forging Process Design, *J. Mat. Process. Technol.*, 2004, **155-156**, p 1583-1589
16. M.C. Cakir, O. Irfan, and K. Cavdar, An Expert System Approach for Die and Mold Making Operations, *Robot. Com-Int. Manuf.*, 2005, **21**, p 175-183